Paper No.
7113

NACE INTERNATIONAL CORROSION 2016 CONFERENCE & EXPO

Relationship between Localized Corrosion and Stress Corrosion Cracking of Nickel Based Alloys in HPHT Oil and Gas Environments

Ramgopal Thodla
DNV USA
5777 Frantz Road
Dublin, OH - 43017

Liu Cao
DNV USA
5777 Frantz Road
Dublin, OH - 43017

Jeffery Hawk
NETL
1450 Queen Avenue SW
Albany, OR 97321-2198

Margaret Ziomek-Moroz
NETL
1450 Queen Avenue SW
Albany, OR 97321-2198

ABSTRACT

Fatigue and fracture performance of UNS N07718 (718) and UNS N07716 (625+) in sour environments over a range of temperatures (300 to 400°F) and chloride concentrations (0.15wt% to 25wt% NaCl). Rising displacement fracture toughness test performed in a range of environments indicated that the fracture toughness was a strong function of chloride concentration and temperature. The initiation fracture toughness values were lower in environment compared to the in-air values. The initiation toughness decreased with increasing chloride concentration and temperature. At a given chloride concentration, the initiation fracture toughness at 400°F was significantly lower than at 300°F or 350°F. Increasing chloride concentration at 400°F led to a sharp decrease in the initiation toughness. Decreasing initiation toughness was associated with increasing intergranular cracking. Increasing temperature and chloride concentration resulted in a decrease in the repassivation potential of IN718. The decrease in repassivation potential was sharp at 400°F. Increasing chloride concentration at 400°F also led to a sharp decrease in the repassivation potential. Similar behavior was observed for 625+. There was no significant effect of the chloride concentration on the corrosion potential. The decrease in fracture toughness coincided with a decrease in the repassivation potential (in particular when the repassivation potential was below the corrosion potential), which suggest that in sour environments at elevated temperatures, the factors that are responsible for stabilizing pit growth also contribute to stabilizing local environments that favor environmentally assisted cracking.

INTRODUCTION

There is a growing trend of increased offshore oil and gas production in recent years. A significant number of the new found fields in recent years have been in deep water and the wells are high pressure/high temperature (HPHT)[1]. The increased water depths combined with extreme HPHT conditions present a significant challenge for various materials. For example, the increased water depth places a significant demand on the strength of the material. The use of conventional material for subsea applications with yield strength (YS) in the range of 70 -100ksi makes it impractical to transport and install the equipment in deep water applications. This has led to the industry to explore high strength steels for these applications. A range of steels can be heat treated to obtain strengths in the

©2016 by NACE International.
Requests for permission to publish this manuscript in any form, in part or in whole, must be in writing to
NACE International, Publications Division, 15835 Park Ten Place, Houston, Texas 77084.
The material presented and the views expressed in this paper are solely those of the author(s) and are not necessarily endorsed by the Association.

range of 120 - 160ksi. However, most of these materials have poor resistance to hydrogen embrittlement. The internal environment of the subsea equipment will experience temperatures in excess of 300°F, with partial pressures of H_2S in the range of 1-2psia coupled with low pH. These environments are extremely aggressive leading to high corrosion rates of steels. The high corrosion rates coupled with hydrogen recombination poisons leads to ingress of atomic hydrogen, which can subsequently lead to cracking due to hydrogen embrittlement. This has led to the need for evaluating and using corrosion resistant alloys (CRA's) like precipitation hardened nickel-based alloys for these applications.

There has been a significant amount of work in the development of precipitation hardened nickel-based alloys in the last 20 years for the oil and gas (O&G) industry[2-10]. The main applications for these materials are rods and tubes for downhole tubing, valves, hangers, loading nipples, tool joints and packers[6]. Precipitation hardened nickel-based alloys contain Cr and Mo, for improving aqueous corrosion resistance[7]. These alloys also contain a significant amount of Ti/Nb/Al additions for formation of γ/γ' precipitates which lead to high strength[7- 8]. These alloys are typically solution annealed, cold worked and aged to form the strengthening precipitates to obtain high strength. The strengthening mechanism in these alloys is due to strain hardening from these precipitates. The precipitates reduce dislocation mobility leading to pinning of dislocations, which is responsible for the high strength in these alloys[7]. However, precipitation of deleterious grain boundary precipitates can lead to significant degradation of environmentally cracking resistance[7-8]. Minor changes in chemistry and heat treatments help prevent/eliminate continuous grain boundary precipitates like carbides/eta/delta phases.

The primary materials that been used in the O&G industry are IN718, IN725, IN925, IN945 and their variants[3,10]. These alloys have strength ranging from 110ksi to 140ksi, which provide significant advantages in terms of weight savings in subsea applications[3]. The primary concern in using these materials in O&G applications is their resistance to EAC in sour environments at elevated temperatures containing CO_2/H_2S and potentially elemental S. The EAC evaluation of these alloys, has been performed in accordance with environments in ISO15156/NACE MR0175[11] or in simulated field conditions that are specified to evaluate fitness for purpose. The precipitation hardened nickel-based alloys are typically evaluated in NACE Level V, VI, and VII environments, which are associated with temperatures greater than 300°F, CO_2, and H_2S content higher than 100psia and NaCl levels of 15wt% and higher[11]. The EAC resistance of these alloys has largely been evaluated using constant load C-ring tests or slow strain rate (SSR) testing. C-ring tests are usually performed by stressing the specimens to a desired stress level (90% to 100% specified minimum yield strength (SMYS) followed by exposing the specimens to the test environment for an extended duration (30 to 90 days)[12]. The evaluation of the material in C-ring tests is qualitative, usually the presence or absence cracking at 10x magnification under an optical microscope. In certain cases if localized corrosion is observed on the surface, cross-sectional metallography is performed to determine if there is cracking associated with the localized corrosion site[12]. Evaluation of material using SSR tests are usually performed by comparing the stress-strain behavior in an inert environment (Air or N_2) with the behavior in the sour environment of interest. The tests are typically performed at strain rate of 4×10^{-6}/s. SSR tests have also been performed in NACE Level V, VI, and VII environments as well as simulated field environments[2,8,14]. A significant amount of work has also been performed in a simulated field environment containing 25wt% NaCl and 0.5wt% acetic acid with 100psia H_2S at various temperatures starting at 250°F[2,6,8]. The susceptibility of the material is evaluated by comparing the elongation to failure, reduction in area, and time to failure in the environment to the values in-air, as well as observation of secondary cracking on the gage section of the specimens. ISO15156/NACE MR0175 Level V, VI, VII test environments do not contain acetic acid (though the lower levels do contain acetic acid), while a number of fitness for service tests have included acetic acid and the results suggest that addition of acetic acid increases the susceptibility to EAC[14]. The reason for the increase in susceptibility is not very clear. The increase in susceptibility could be related to a decrease in pH in the presence of acetic acid. It is also likely that the presence of acetic acid could alter the repassivation behavior in the presence of sour environments at elevated temperatures in nickel-based alloys and thus affect the cracking susceptibility.

©2016 by NACE International.
Requests for permission to publish this manuscript in any form, in part or in whole, must be in writing to
NACE International, Publications Division, 15835 Park Ten Place, Houston, Texas 77084.
The material presented and the views expressed in this paper are solely those of the author(s) and are not necessarily endorsed by the Association.

The lack of detailed understanding of the role of various environmental parameters on the susceptibility to cracking is due to limited electrochemical data in sour environments. This is particularly true of nickel-based alloys in sour environments at elevated temperatures. Limited electrochemical data exist on stainless steels and nickel-based alloys at elevated temperatures (>300°F). These results suggest that pitting and repassivation potentials are independent of temperature at temperatures above 300°F 400°F depending on the chemistry of the alloy[15,16]. The presence of limited amount of sulfides in solution does not appear to alter the pitting and repassivation potentials. It has also been found that the morphology of pitting changes from deep and narrow pits to shallow and broad in nature[17]. The susceptibility to cracking is significantly higher at potentials above the repassivation potential for stainless steels and nickel-based alloys in chloride containing environments. It has been suggested, the conditions needed to maintain critical crack tip chemistry are met at potentials above the repassivation potential but not below it[18,19]. The critical chemistry at the crack tip in combination with the appropriate crack tip strain rate conditions would lead to high crack growth rates. As the potential decreases below the repassivation potential, the conditions needed to maintain the critical chemistry at the crack tip are not met and thus lead to a decrease in the crack growth rate[18]. In order to develop a complete understanding of the behavior of cracking susceptibility it would be important to characterize the electrochemical behavior of the nickel-based alloys in a range of sour environments as a function of temperature to co-relate with the EAC behavior.

The results of the material evaluation described above are performed using C-ring and SSR and typically result in pass/fail of the materials of interest in the testing environment. These results have been found to be satisfactory in stress based designs. However, there is also a growing trend in the industry to use a fracture mechanics based approach for design as opposed to a stress based design approach. A fracture mechanics based design approach can optimize the design process and take advantage of the improved properties of advanced materials like precipitation hardened nickel-based alloys. It is essential to have crack growth and fracture toughness data of the nickel-based alloys in order to support the new design approach.

EXPERIMENTAL

The materials tested as part of the test program were Alloy 718 and Alloy 625+. The chemistry of materials tested is shown in Table 1. Rising displacement fracture toughness tests were performed using compact tension specimens in the L-R orientation. The compact tension (CT) specimens had a B = 0.25” and W = 1” and had an a/W of 0.6.

Rising displacement fracture toughness measurements were performed in-air at all of the temperatures investigated to serve as a baseline against which to compare the environmental test results. The test matrix for the rising displacement fracture toughness tests for 718 and 625+ is shown in Table 2. Tests were performed on 718 as a function of chloride concentration at 300°F, 350°F, and 400°F. The effect of acetic acid was investigated at 400°F across a range of chloride concentrations. The effect of K-rate on the fracture toughness behavior was investigated at 400°F in 25wt% NaCl. 625+ was investigated at 400°F as a function of chloride concentration and acetic acid at 400°F. The effect of K-rate on the fracture toughness behavior was investigated at 400°F in 25wt% NaCl.

Electrochemical polarization scans tests were performed on 718 and 625+ as a function of chloride concentration, H_2S levels as a function of temperature. The test matrix of the electrochemical tests performed is shown in Table 3. Electrochemical measurement of potentiodynamic polarization followed by potentiostatic hold to pass sufficient charge and subsequently potentiodynamic polarization scan (PDP-PS-PDP) test was performed after overnight OCP monitoring. Forward potentiodynamic scan started from -100 mV vs. OCP to a potential at which abrupt anodic current was observed. Then test switched to potentiostatic holding at that potential to ensure at least 2 C/cm^2 total charge density. In

©2016 by NACE International.
Requests for permission to publish this manuscript in any form, in part or in whole, must be in writing to
NACE International, Publications Division, 15835 Park Ten Place, Houston, Texas 77084.
The material presented and the views expressed in this paper are solely those of the author(s) and are not necessarily endorsed by the Association.

backward potentiodynamic scan, it started from present potential towards negative direction until -100 mV vs. OCP. Both forward and backward scan were conducted at a slow scan rate of 0.167 mV/s as per ASTM G61. The criterion on initiation of localized corrosion in the presence of H_2S was discussed in the next part. Solution resistance was obtained from electrochemical impedance spectroscopy (EIS) before and after PDP-PS-PDP measurement and the post-measurement IR compensation was applied on the electrochemical results, when NaCl concentration was relatively low. Electrochemical tests in H_2S containing environments were performed at two different chloride concentrations (20wt% and 0.2wt%) across all temperatures on 718. Subsequently tests were performed on 718 and 625+ as a function of chloride concentration (corresponding to the concentrations at which the rising displacement fracture toughness tests were performed) in the absence of H_2S.

A platinized niobium coil was used as counter electrode, which was embedded in a perforated polytetrafluroethylene (PTFE) tube to avoid galvanic contact with the autoclave body. The reference electrode was a custom built pressure balanced external electrode for HT/HP conditions. It was based on Ag/AgCl electrode which was operating at room temperature by a water cooling jacket. The reference assembly has a potential of -44 mV vs. saturated calomel electrode (SCE) at room temperature. The reference assembly was checked against SCE before and after tests to ensure its proper functionality. All the potentials of the tests are reported with respect to this customized reference electrode (RE) at testing temperature.

RESULTS AND DISCUSSION

Fracture Toughness Behavior of UNSN07718

The results of the J-R curves for 718 performed at different temperatures is shown in Figure 1. The results of the J-R curves at 300°F show that while there is some effect of the environment on the R-curve behavior, there is no significant effect of the chloride concentration on the R-curve behavior. At the higher temperature of 350°F there is some difference in the effect of chloride concentration at 0.2wt% and 20wt% NaCl, with the R-curve at 20wt% NaCl being lower than at 0.2wt% NaCl. The results at 400°F clearly indicate that there is a strong effect of chloride concentration with the data at 25wt% NaCl being significantly lower than the data at 0.25wt% and 2.5wt% NaCl. There is a slight effect of acetic acid addition at 25wt% NaCl though it doesn't appear to be significant.

Initiation toughness as a function of chloride concentration is shown in Figure 2. The results appear to indicate that the initiation toughness are high ~120MPa√m at low chloride concentrations (less than 2.5wt% NaCl) independent of temperature. At higher chloride concentrations of 20wt% NaCl at 350°F there appears to be a decrease in the initiation toughness to about 100MPa√m, while at 400F and 25wt% NaCl there is a substantial decrease in the initiation toughness to about 50MPa√m. In the presence of 0.5wt% acetic acid at 400°F doesn't appear to have any significant effect on the initiation toughness. At the low chloride concentrations the initiation toughness is high even in the presence of 0.5wt% acetic acid and appears to drop sharply in 25wt% NaCl similar to the observation in the absence of 0.5wt% acetic acid. The value of the initiation toughness in the presence of 0.5wt% acetic acid is slightly lower than without, indicating that there is a synergistic effect of acetic acid and chloride concentration.

The crack growth rate (CGR) behavior as function of chloride concentration at different temperatures is shown in Figure 3. The results of the CGR are consistent with the measurements of K_{th} with low values of CGR ~4×10^{-6} mm/s at low chloride concentrations (upto 2.5wt% NaCl) and lower temperatures (300°F and 350°F). At 400°F in 25wt% NaCl, the CGR increases by more than 10 times to about 8×10^{-5} mm/s. The presence of 0.5wt% acetic acid appears under these conditions appears to increase the CGR by about 3 times compared to the case without acetic acid to about 2×10^{-4} mm/s. These observations are consistent with the observations of lower K_{th} in the presence of 0.5wt% acetic acid in the presence of 25wt% NaCl.

©2016 by NACE International.
Requests for permission to publish this manuscript in any form, in part or in whole, must be in writing to
NACE International, Publications Division, 15835 Park Ten Place, Houston, Texas 77084.
The material presented and the views expressed in this paper are solely those of the author(s) and are not necessarily endorsed by the Association.

SEM observations of the fracture surfaces on samples tested at 400°F as a function of chloride are shown in Figure 4. The SEM micrographs show clear evidence of ductility at 0.25wt% NaCl. At 2.5wt% NaCl, while the majority of the fracture surface exhibits evidence of ductility, there are some regions exhibiting evidence of quasi cleavage/intergranular cracking. In 25wt% NaCl there is clear evidence of quasi cleavage and evidence of transgranular cracking. These observations are consistent with the observations of sharp decrease in the K_{th} and increase in CGR at 25wt% NaCl.

The effect of K-rate on the fracture toughness behavior of 718 was investigated at 400F in the presence of 25wt% NaCl. The results of the fracture toughness tests as function of K-rate are shown in Figure 5. The effect of K-rate in the range of 0.05Nmm$^{-3/2}$/s to 0.005Nmm$^{-3/2}$/s on the initiation toughness is relatively small with the initiation toughness changing from about 10N/mm to about 5N/mm. However, the J_{1mm} and $J_{maxload}$ decrease rather sharply at 0.005Nmm$^{-3/2}$/s suggesting a substantial decrease in the resistance to crack growth at the lowest K-rate tested.

Fracture Toughness Behavior of UNSN07716

The J-R curve behavior of 625+ as a function of chloride concentration, acetic acid, and K-rate is shown in Figure 6. The data clear indicates that there is a strong effect to chloride concentration on the R-curve behavior at 25wt% NaCl. However, at lower chloride concentrations while there is a drop in the R-curve behavior from the in-air performance there appears to be no significant differences between 0.25wt% NaCl and 2.5wt% NaCl. There also appears to be no significant difference in the R-curve behavior with the addition of 0.5wt% acetic acid at chloride concentrations of 2.5wt% NaCl or lower. The addition of 0.5wt% acetic acid at 25wt% NaCl doesn't appear to alter the R-curve behavior in any significant manner. The effect of K-rate was explored at 25wt% NaCl (Figure 6) and the results suggest that with decreasing K-rate, the slope of the R-curve decreases.

The results of the R-curve behavior are summarized in Figure 7. The initiation toughness for cracking indicated by $J_{0.2mm}$ decreases 120N/mm to about 75N/mm as the chloride concentration increases from 2.5wt% NaCl to 25wt% NaCl. The values of $J_{0.2mm}$ are significantly higher than those measured on 718 under similr conditions. This is consistent with the higher resistance of 625+ in sour environments compared to 718. There is no significant difference in the initiation toughness at 0.25wt% NaCl and 2.5wt% NaCl. The addition of acetic acid appears to have no effect on the initiation toughness at any chloride level investigated. The CGR measured at K_J of 133MPa√m at low chloride concentrations (less than 2.5wt% NaCl) are in the range of 2×10^{-6} mm/s which is about 10 times lower than value measured for 718 under similar conditions. The CGR increases at the high chloride concentration of 25wt% NaCl by about 5 times 1×10^{-5} mm/s and is consistent with the observed decrease in the initiation toughness $J_{0.2mm}$. The value of CGR is also about 10 times lower than the corresponding CGR of 718 under similar conditions. There is no discernable effect of acetic on the CGR at any chloride level and is consistent with the effect of acetic acid on the initiation toughness. It is interesting to note that the increase in CGR from the low chloride to high chloride concentration for 625+ is not as significant as observed in case of 718. This is likely associated with lower decrease in the initiation toughness for 625+ at the high chloride concentration compared to 718.

The effect of K-rate on the fracture toughness parameters is shown in Figure 8. The results indicate with decreasing K-rate the initiation toughness decreases from about 100N/mm to about 50N/mm as the K-rate decreases from 0.16Nmm$^{-3/2}$/s to 0.005Nmm$^{-3/2}$/s. This behavior is similar to that of 718, though the initiation values are significantly higher. The values of J_{1mm} and $J_{maxload}$ also decrease substantially with K-rate by about a 2.5 times in the range of K-rates tested. At the lowest K-rate investigated the $J_{maxload}$ is substantially closer to the initiation toughness suggesting that the resistance to crack growth is much lower at the lower K-rate.

The SEM micrographs of the 625+ as function of chloride concentration are shown in Figure 9. The micrographs indicate that the fracture surfaces in 0.25wt% NaCl and 2.5wt% NaCl exhibit extensive ductility with no evidence of quasi cleavage. There is some evidence of transgranular cracking at high

©2016 by NACE International.
Requests for permission to publish this manuscript in any form, in part or in whole, must be in writing to
NACE International, Publications Division, 15835 Park Ten Place, Houston, Texas 77084.
The material presented and the views expressed in this paper are solely those of the author(s) and are not necessarily endorsed by the Association.

chloride concentration of 25wt% NaCl. The extent of transgranular cracking is substantially lower than in 718 indicating consistent with the values of K_{th} for crack initiation.

Electrochemical Behavior of UNSNN07718 and UNSN07716

The electrochemical behavior of 718 was investigated as function of chloride concentration with and without H_2S at 400°F. The results of the polarization scans are shown in Figure 10. The polarization curves in the presence of H_2S at low chloride concentrations of 0.2wt% NaCl indicated a high current density on the forward and backward scans likely associated with the oxidation/reduction of H_2S. This made it difficult to uniquely identify the repasssivation potential of 718 in the presence of H_2S in dilute chloride environments. This is likely due to the higher solubility of H_2S in the lower chloride environments, which leads to increased oxidation/reduction currents which mask the currents associated with metal dissolution reactions. The influence of oxidation/reduction reactions is not as pronounced at the higher chloride concentration likely due to the decreased solubility of H_2S at the higher chloride concentrations. In order to be able to quantify the effect of the chloride concentration electrochemical scans were performed as a function of chloride in the absence of H_2S and the effect of chloride concentration is evident in Figure 10. The repassivation potential decreases from about -100mV SHE to about -350mV SHE as the concentration of chloride increases from 0.25wt% NaCl to 25wt% NaCl. The effect of temperature on the repassivation potential is shown in Figure 11. The repassivation potential decreases from about -220mV SHE to about -350mV SHE at high chloride concentration as the temperature increases from 300°F to 350°F. A comparison of the electrochemical behavior of 625+ and 718 is shown in Figure 12. The results indicate that at all temperatures in the range of 300F to 400F, the repassivation potential of 625+ is about 80 to 100mV SHE higher than that of 718 in 20wt% NaCl concentration.

The repassivation behavior of nickel based alloys in high chloride environments is determined by the pit chemistry and the ability to maintain a critical concentration of metal ions at the bottom of a growing pit. The critical concentration of metal ions needed to maintain stable pits has been shown to about 80% of saturation in stainless steels at room temperature in chloride containing solutions. While the pit bottom chemistry in nickel based alloys at high temperatures has not been studied it is reasonable to assume that a certain fraction of saturation of metal ions is needed at the pit bottom. The potentials above which the critical concentration of ions can be sustained will favor localized corrosion while at potentials below it localized corrosion cannot be sustained. Earlier work on stainless steels and nickel based alloys has shown that the repassivation potential represents the transition potential associated with pit stability. The chemistry in a crack is notionally similar to that of pit in that it is an occluded environment, which is concentrated in metal ions and has a low pH due to the hydrolysis of metal ions. Similar to a pit bottom fresh metal is exposed by a combination of crack growth as well as straining at the crack tip in the rising displacement tests.

It is postulated that in austenitic steels and nickel based alloys, when a critical crack tip strain rate is established stable cracking can initiate and grow. The critical strain rate is a combination of establishing the critical chemistry and the loading conditions at the crack tip. The onset of stable cracking is associated with the strain rate at the crack tip exceeding the threshold crack tip strain rate. This hypothesis would suggest that the electrochemical processes associated with the onset of localized corrosion and stress corrosion cracking are similar. This is schematically illustrated in Figure 13.

The rising displacement tests performed to investigate the onset of stress corrosion cracking and subsequent crack growth were all performed at the OCP in H_2S containing environments. The measured K_{th} and CGR were related to the repassivation potentials were estimated in the absence of H_2S in particular to facilitate comparison at the low chloride concentrations. It is expected that if the corrosion potential is close to or above the repassivation the material would be susceptible to localized corrosion and hence also likely to be susceptible to stress corrosion cracking. However, if the corrosion

©2016 by NACE International.
Requests for permission to publish this manuscript in any form, in part or in whole, must be in writing to
NACE International, Publications Division, 15835 Park Ten Place, Houston, Texas 77084.
The material presented and the views expressed in this paper are solely those of the author(s) and are not necessarily endorsed by the Association.

potential is significantly below the repassivation potential the likelihood of localized corrosion decreases significantly and under these conditions it is also likely more resistant to stress corrosion cracking. The corrosion potential can be influenced by the presence of H_2S both due to modifications to the passive as well as due to the oxidation/reduction of H_2S. The difference between the corrosion potential and repassivation potential serves as a measure of susceptibility to localized corrosion. The relationship between this difference and the K_{th} and CGR for 718 and 625+ over the entire rate of conditions tested is shown in Figure 14. The K_{th} decreases sharply and the CGR increases for 718 when the repassivation potential is close to the corrosion potential, which corresponds to the 400°F, 25wt% NaCl condition. In all other conditions for 718 the repassivation potential is significantly higher than the corrosion potential and correspondingly is associated with conditions where the K_{th} increases and CGR decreases. The behavior of 625+ is similar to the behavior observed in 718. As the corrosion potential is closer to the repassivation potential the K_{th} decreases and the CGR increases. 625+ is more highly alloyed in Cr and Mo and has significantly higher resistance to localized corrosion and is reflected in the higher repassivation potential and correspondingly higher difference between the repassivation potential and corrosion potential. This also corresponds to a higher value of K_{th} and lower CGR for 625+ as seen in Figure 14.

The above results suggest that there is a strong correlation between the susceptibility to localized corrosion and the stress corrosion cracking behavior of nickel based alloys in the sour environments investigated.

SUMMARY

The current work investigated the effect of environmental variables on the stress corrosion cracking behavior of high strength nickel based in HPHT applications. The results indicate that:

1. Chloride concentration has little effect on the stress corrosion cracking behavior at 300°F, while at 400°F there is a strong effect of chloride concentration, with low values of K_{th} at high chloride concentrations on 718. The behavior of 625+ is similar though the decrease in the K_{th} is lower than for 718.
2. There is little effect of acetic acid addition at low chloride concentration across the range of temperatures investigated. At 400°F in high chloride concentration in the presence of 0.5wt% acetic acid the K_{th} decreases and the CGR increases on 718, while there was no discernable effect of acetic acid on the behavior of 625+.
3. The effect of K-rate was investigated on both 718 and 625+ at 400°F and 25wt% NaCl indicates that K_{th} decreases with decreasing K-rate.
4. The resistance to localized corrosion decreases with increasing chloride concentration and temperature as measured via the repassivation potential for 718. 625+ which is more highly alloyed with Cr and Mo exhibits significantly higher resistance to localized corrosion.
5. The stress corrosion cracking behavior measured via K_{th} and CGR correlate with the susceptibility to localized corrosion measured by (E_{rp}-OCP). Increasing resistance to localized corrosion is associated with higher values of K_{th} and lower CGR. 625+ has higher K_{th} and lower CGR compared to 718 which is consistent with the higher E_{rp}-OCP for 625+ compared to 718.

REFERENCES

1. HPHT Wells Summit 2010 (hphtwells.com).
2. Sarwan Manan, “Alloys 945 and its Derivative – Higher Strength products for Oil and Gas”, Paper No. 10310, NACE 2010.
3. Sarwan Manan, “Corrosion Resistance and Mechanical Properties of a 140ksi minimum Alloy 945X for HPHT Applications”, Paper C2012-1393, NACE 2012.
4. Edward L. Hibner, Curtis S. Tansen “Corrosion Resistant OCTG’s for a range of Sour Gas Service Conditions”, Paper 00149, NACE 2010.

©2016 by NACE International.
Requests for permission to publish this manuscript in any form, in part or in whole, must be in writing to
NACE International, Publications Division, 15835 Park Ten Place, Houston, Texas 77084.
The material presented and the views expressed in this paper are solely those of the author(s) and are not necessarily endorsed by the Association.

5. Edward L. Hibner, and Curtis S. Tansen "Corrosion Resistant OCTG's and Matching Age-Hardenable Bar Products in a range of Sour Gas Service Conditions," Paper No. 01102, NACE 2001.
6. Rainer Behrens and D. C. Agarwal "Laboratory testing of age-hardenable alloys 925 and 718 in sour gas environments," Paper No. 05103, NACE 2005.
7. Sarwan Manan, Ed Hibner, and Brett Puckett, "Physical metallurgy of Alloys 718, 725, 725HS, 925 for Service in Aggressive Corrosive Environments", Paper No. 03126, NACE 2003.
8. Rashmi B. Bhavsar, Ed Hibner, "Evaluation of Corrosion Testing Techniques for Selection of Corrosion Resistant Alloys for Sour Gas Service," Paper No. 59, NACE 1996.
9. Ed Hibner, "High Strength Corrosion Resistant Nickel Base Alloy 725HS for Sever Sour Oil and Gas Field Application", Paper No. 03125, NACE 2003.
10. Luca Foroni, and Carlo Malara, "High Strength and Corrosion Resistant Superalloys for Oil Gas," Paper No. 11116, NACE 2011.
11. NACE MR0175/ISO 15156-1 - "Petroleum and natural gas industries - Materials for use in H_2S-containing Environments in oil and gas production."
12. NACE TMO177 - "Laboratory Testing of Metals for Resistance to Sulfide Stress Cracking and Stress Corrosion Cracking in H_2S Environments."
13. M. Ueda, H. Amaya, and H. Okamoto, "Economical Nickel Base Alloy for Sour Environment at Elevated Temperature," Paper No. 25, NACE 1997.
14. M. Ueda, and Takeo Kudo, "Evaluation of SCC Resistance of CRA's in Sour Service", Paper No. 2, NACE 1991.
15. L. F. Lin, G. Cragnolio, Z. Szklarska-Smialowska, D. D. MacDonald, Corrosion, Vol. 37, No. 11, p. 616, 1981.
16. P. L. Andresen, "The Effects of Aqueous Impurities on Intergranular Stress Corrosion Cracking of Sensitized Type 304 Stainless Steel", EPRI Report No. NP-3384, Electric Power Research Institute, Palo Alto, CA, November, 1983.
17. G. Cragnolino, "NACE - 9: Advances in Localized Corrosion", H. Isaacs, U. Bertocci, J. Kruger, and S. Smialowska, 1987.
18. G. A. Cragnolino, D. S. Dunn, Y. M. Pan, and N. Sridhar, "The Critical Potential for Stress Corrosion Cracking of Fe-Ni-Cr Alloys and Mechanistic Implications", Chemistry and Electrochemistry of Corrosion and Stress Corrosion Cracking: A Symposium Honoring the Contributions of R. W. Staehle. 2001 TMS Annual Meeting.
19. G. Cragnolino, D.S. Dunn, and N. Sridhar, "Environmental Factors in the Stress Corrosion Cracking of Type 316L Stainless Steel and Alloy 825 in Chloride Solutions," Corrosion Vol. 52, No. 3, p.194-203.

TABLES

Table 1
Chemistry of 718 and 625+ tested in this program.

Material	Ni	Cr	Fe	Mo	Nb	Al	Ti	Mn	Si	C	Co	Cu	Ta	P	S	B	Pb
718	52.66	18.34	19.18	3	4.96	0.49	0.95	0.05	0.06	0.03	0.04	0.04	0.01	0.006	0.001	0.003	0.0002
	Ni	Cr	Fe	Mo	Nb+Ta	Al	Ti	Mn	Si	C	Ta	Cu	Mg	P	S	B	Pb
625+	60.81	21.31	4.89	7.99	3.4	0.21	1.26	0.02	0.04	0.008	(a)	0.01	0.001	0.001	0.001	0.003	0.0003

Table 2
Test matrix of rising displacement fracture toughness tests performed on 718 and 625+.

©2016 by NACE International.
Requests for permission to publish this manuscript in any form, in part or in whole, must be in writing to
NACE International, Publications Division, 15835 Park Ten Place, Houston, Texas 77084.
The material presented and the views expressed in this paper are solely those of the author(s) and are not necessarily endorsed by the Association.

Test Matrix for 718					
p_{CO2} (psia)	p_{H2S} (psia)	NaCl (wt%)	Acetic Acid (wt%)	K-rate ($Nmm^{-3/2}/s$)	Temperature (F)
200	100	15	0	0.016	300
200	100	0.15	0	0.016	300
500	100	20	0	0.016	350
500	100	0.2	0	0.016	350
500	100	25	0	0.05/0.016/0.005	400
500	100	2.5	0	0.016	400
500	100	0.25	0	0.016	400
500	100	25	0.5	0.016	400
500	100	2.5	0.5	0.016	400
500	100	0.25	0.5	0.016	400
Test Matrix for 625+					
p_{CO2} (psia)	p_{H2S} (psia)	NaCl (wt%)	Acetic Acid (wt%)	K-rate ($Nmm^{-3/2}/s$)	Temperature (F)
500	100	25	0	0.05/0.016/0.005	400
500	100	2.5	0	0.016	400
500	100	0.25	0	0.016	400
500	100	25	0.5	0.016	400
500	100	2.5	0.5	0.016	400
500	100	0.25	0.5	0.016	400

Table 3
Test matrix of the electrochemical polarization scans performed on 718 and 625+.

Test Matrix for 718					Test Matrix for 625+				
p_{CO2} (psia)	p_{N2} (psia)	p_{H2S} (psia)	NaCl (wt%)	Temperature (F)	p_{CO2} (psia)	p_{N2} (psia)	p_{H2S} (psia)	NaCl (wt%)	Temperature (F)
200	0	100	20	300					
200	0	100	0.2	300					
200	100	0	15	300					
200	100	0	0.15	300					
500	0	100	20	350					
500	0	100	0.2	350					
500	100	0	20	350					
500	100	0	0.2	350					
500	0	100	20	400					
500	0	100	0.2	400					
500	100	0	25	400	500	100	0	25	400
500	100	0	2.5	400	500	100	0	2.5	400
500	100	0	0.25	400	500	100	0	0.25	400

FIGURES

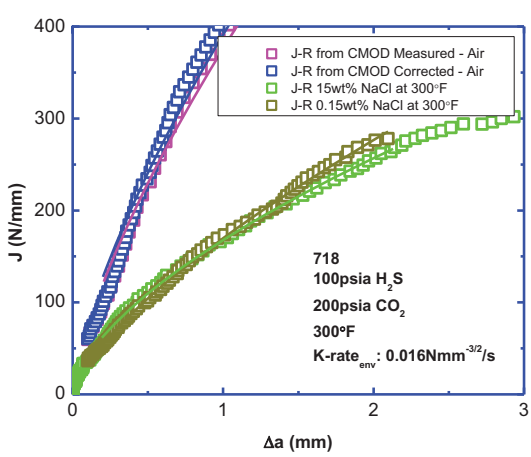

a) 300°F

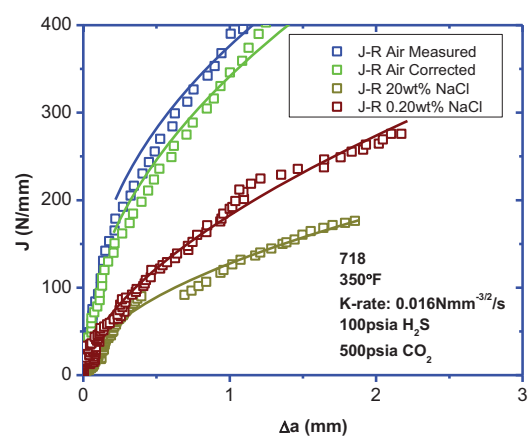

b) 350°F

©2016 by NACE International.
Requests for permission to publish this manuscript in any form, in part or in whole, must be in writing to
NACE International, Publications Division, 15835 Park Ten Place, Houston, Texas 77084.
The material presented and the views expressed in this paper are solely those of the author(s) and are not necessarily endorsed by the Association.

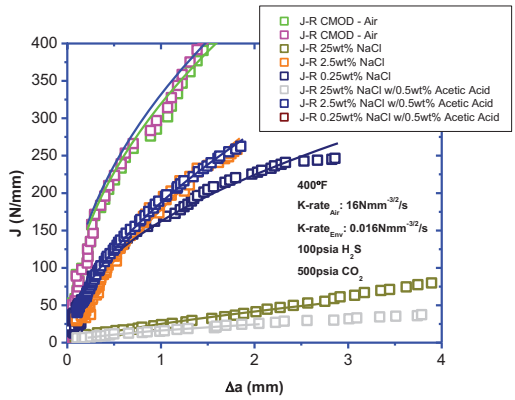

c) 400°F

Figure 1: J-R curves of 718 at 300°F, 350°F, and 400°F as a function of chloride concentration.

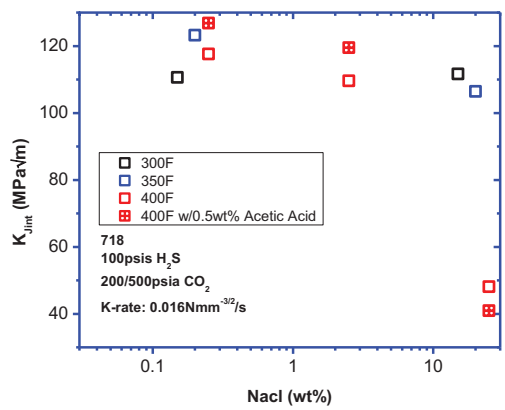

Figure 2: Summary of initiation toughness and R-curve parameters for 718 at 300°F, 350°F, and 400°F as a function of chloride concentration.

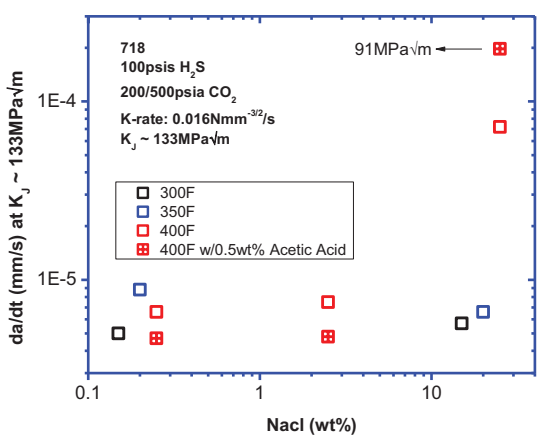

©2016 by NACE International.
Requests for permission to publish this manuscript in any form, in part or in whole, must be in writing to
NACE International, Publications Division, 15835 Park Ten Place, Houston, Texas 77084.
The material presented and the views expressed in this paper are solely those of the author(s) and are not necessarily endorsed by the Association.

Figure 3: Summary of initiation toughness and R-curve parameters for 718 at 300°F, 350°F, and 400°F as a function of chloride concentration.

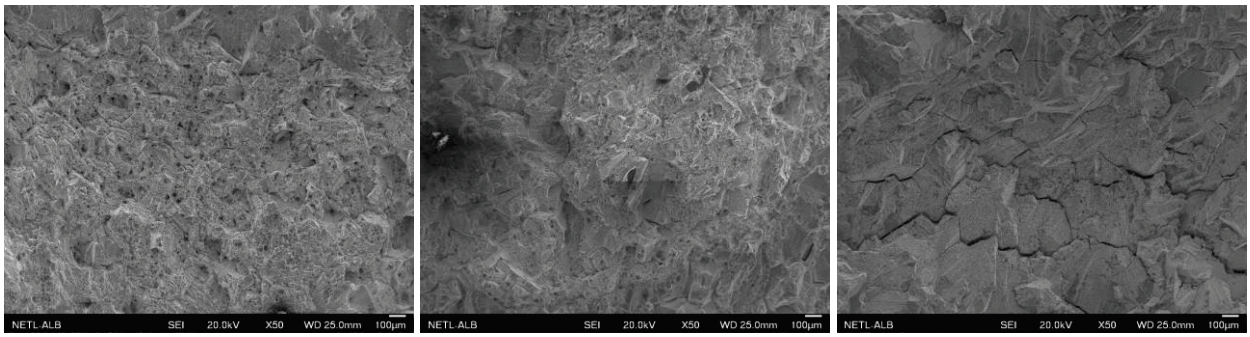

0.25wt% NaCl 2.5wt% NaCl 25wt% NaCl

Figure 4: SEM micrographs of 718 at tested at 400°F as a function of chloride concentration.

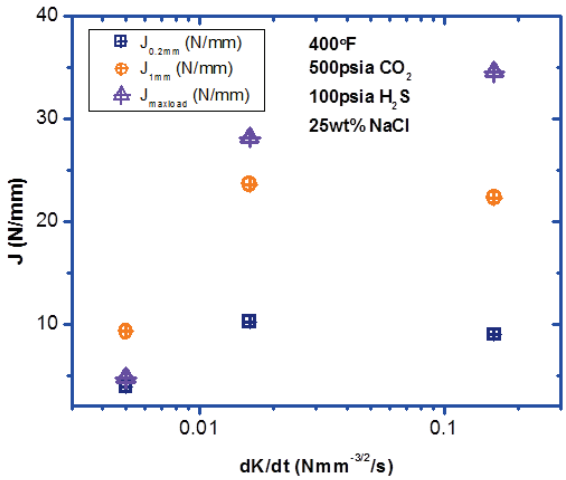

Figure 5: Effect of K-rate on the fracture toughness behavior of 718 at 400°F in the presence of 25wt% NaCl.

©2016 by NACE International.
Requests for permission to publish this manuscript in any form, in part or in whole, must be in writing to
NACE International, Publications Division, 15835 Park Ten Place, Houston, Texas 77084.
The material presented and the views expressed in this paper are solely those of the author(s) and are not necessarily endorsed by the Association.

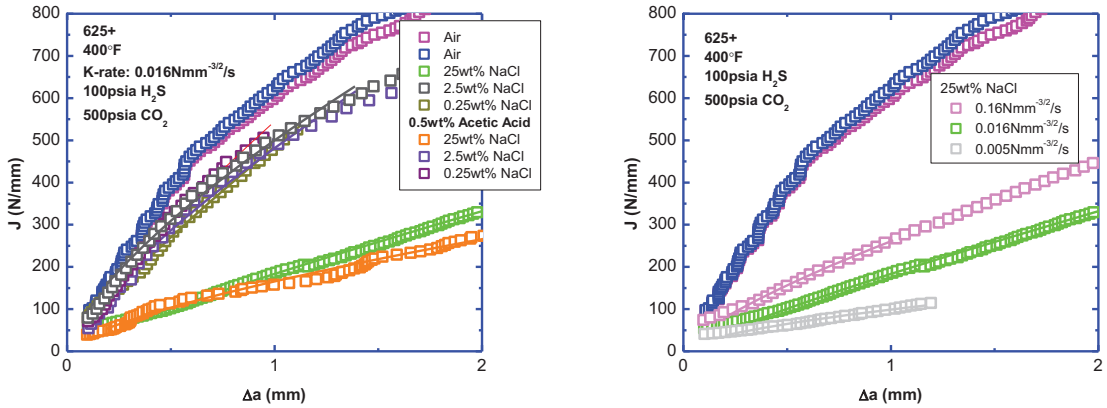

Figure 6: Effect of chloride concentration, acetic acid and K-rate on the fracture toughness behavior of 625+ at 400°F.

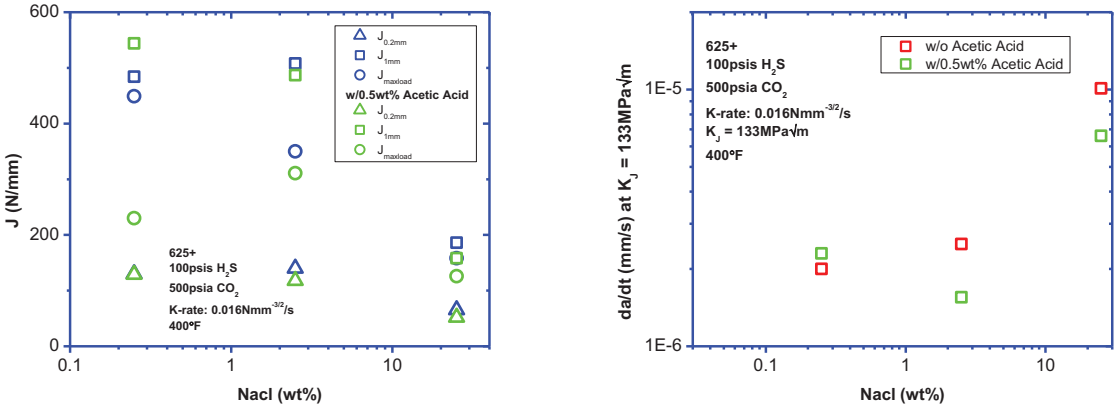

Figure 7: Effect of chloride concentration, and acetic acid on the fracture toughness behavior of 625+ at 400°F.

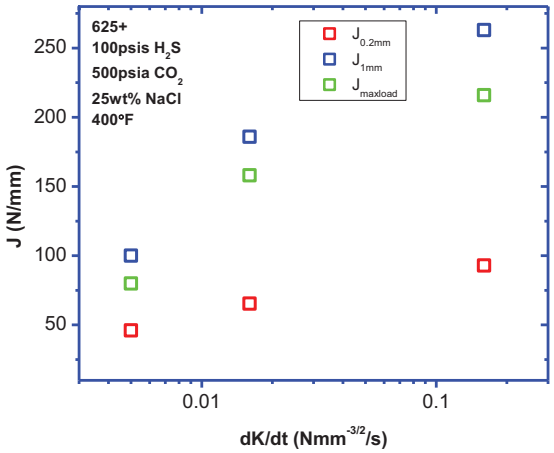

©2016 by NACE International.
Requests for permission to publish this manuscript in any form, in part or in whole, must be in writing to
NACE International, Publications Division, 15835 Park Ten Place, Houston, Texas 77084.
The material presented and the views expressed in this paper are solely those of the author(s) and are not necessarily endorsed by the Association.

Figure 8: Effect of K-rate on the fracture toughness behavior of 625+ at 400°F in 25wt% NaCl.

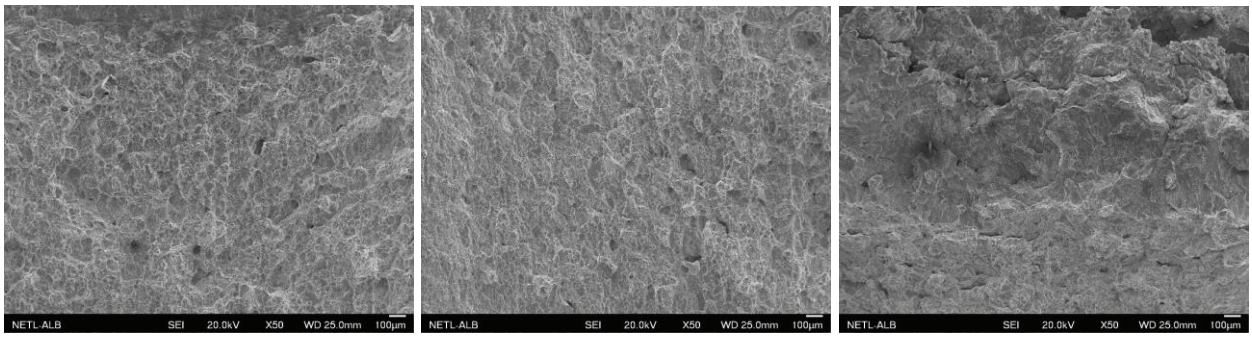

0.25wt% NaCl 2.5wt% NaCl 25wt% NaCl

Figure 9: SEM micrographs of 625+ tested as function of chloride concentration at 400°F.

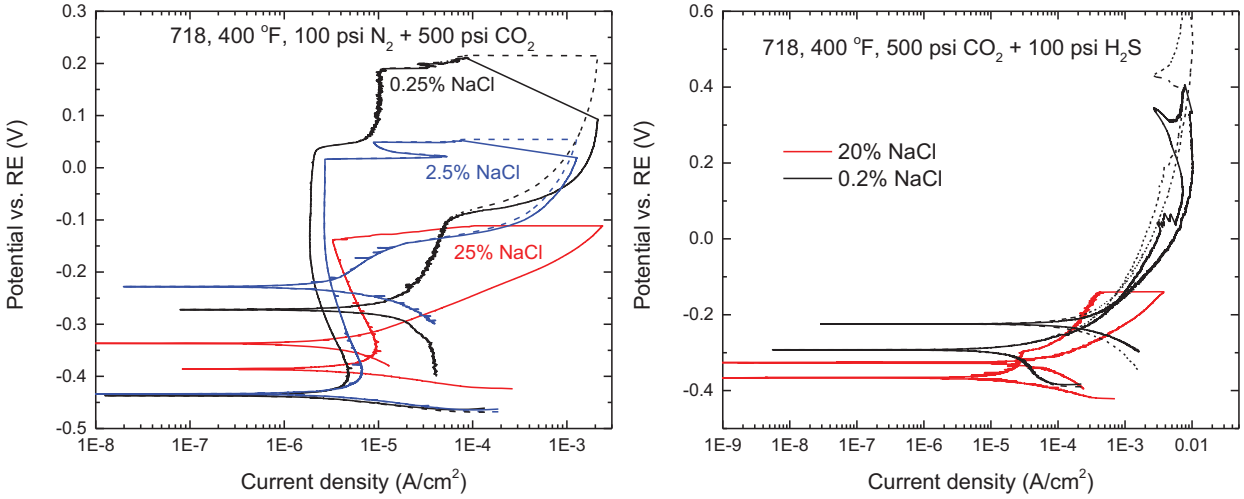

Figure 10: Electrochemical polarization scans on 718 as function of chloride concentration with and without H_2S at 400°F.

©2016 by NACE International.
Requests for permission to publish this manuscript in any form, in part or in whole, must be in writing to
NACE International, Publications Division, 15835 Park Ten Place, Houston, Texas 77084.
The material presented and the views expressed in this paper are solely those of the author(s) and are not necessarily endorsed by the Association.

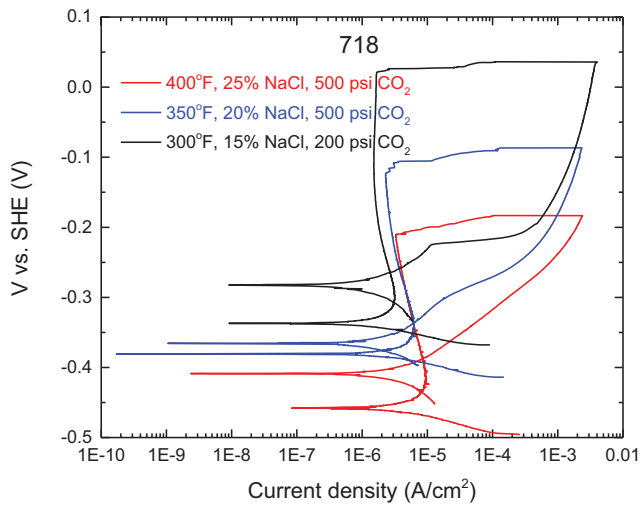

Figure 11: Electrochemical polarization scans on 718 as temperature in the absence of H_2S.

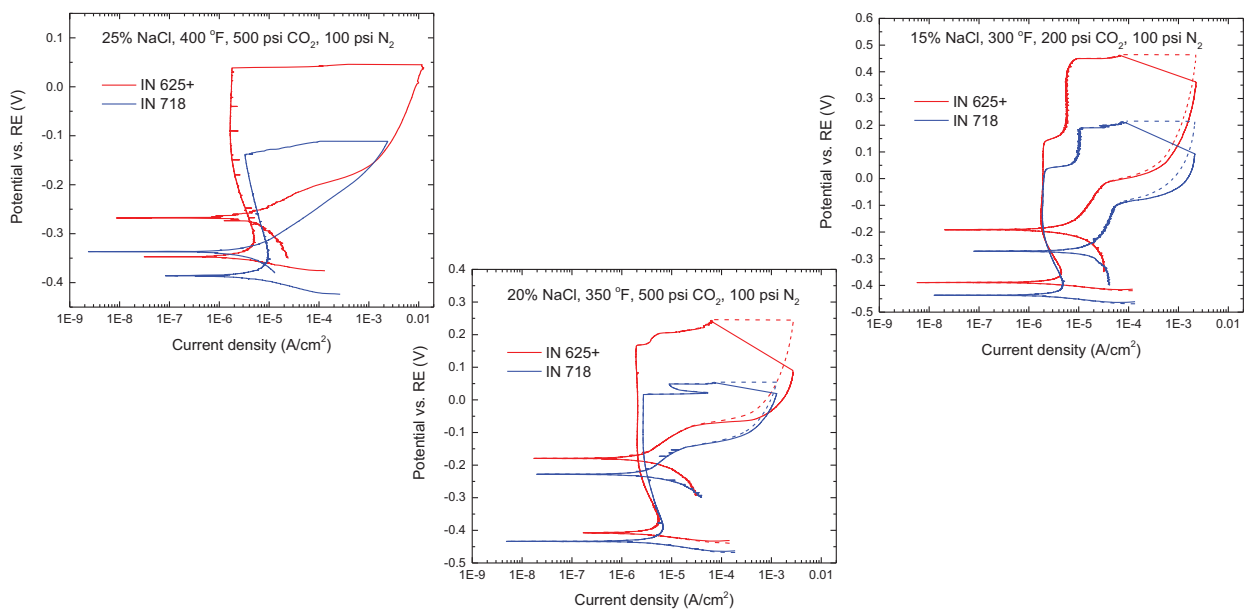

Figure 12: Comparison of the electrochemical behavior of 625+ and 718 in 20wt% NaCl as a function of temperature.

©2016 by NACE International.
Requests for permission to publish this manuscript in any form, in part or in whole, must be in writing to
NACE International, Publications Division, 15835 Park Ten Place, Houston, Texas 77084.
The material presented and the views expressed in this paper are solely those of the author(s) and are not necessarily endorsed by the Association.

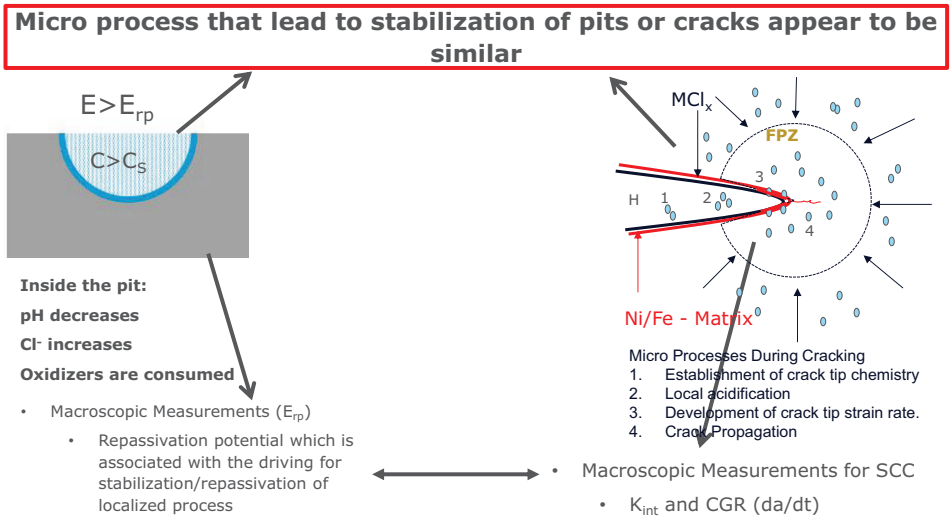

Figure 13: Schematic illustration of the micro processes associate with localized corrosion and their likely relationship with stress corrosion cracking phenomenon.

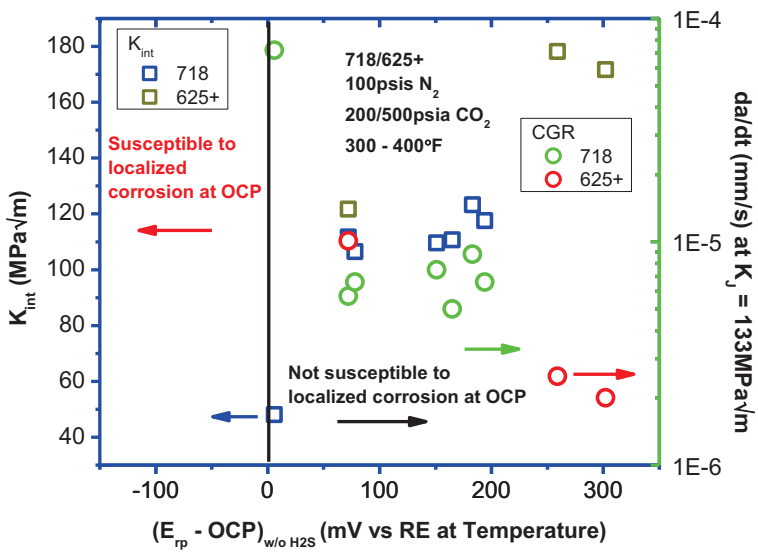

Figure 14: Correlation between K_{th} and CGR as a function of the difference between the repassivation potential and corrosion potential.

©2016 by NACE International.
Requests for permission to publish this manuscript in any form, in part or in whole, must be in writing to
NACE International, Publications Division, 15835 Park Ten Place, Houston, Texas 77084.
The material presented and the views expressed in this paper are solely those of the author(s) and are not necessarily endorsed by the Association.